Eur. Phys. J. C 20, 93–103 (2001)
Digital Object Identifier (DOI) 10.1007/s100520100659

THE EUROPEAN PHYSICAL JOURNAL C

Rescattering effects in ϕ photoproduction

A.V. Anisovich[1], U. Thoma[2]

[1] Petersburg Nuclear Physics Institute, 188350 Gatchina, Russia
[2] Institut für Strahlen- und Kernphysik, Universität Bonn, 53115 Bonn, Germany

Received: 14 September 2000 / Revised version: 1 February 2001 /
Published online: 12 April 2001 – © Springer-Verlag 2001

Abstract. We calculate the contribution from rescattering of K^+K^- pairs produced by photoproduction of $\Lambda(1520)K^+$ to the photoproduction of ϕ mesons. The photoproduction of ϕ mesons is presently a hot topic due to the possibility that an intrinsic hidden strangeness contribution in the nucleon flavor wave function may be revealed in this process, and due to the possibility that the structure of scalar mesons could be accessible experimentally via $S-P$ interference in the K^+K^- system. We show that rescattering makes an important contribution to ϕ photoproduction which could – if neglected – mislead the interpretation of the forthcoming high precision data.

1 Introduction

The non-relativistic quark model has met with considerable success, with more success than one might believe such a naive model could have. The existence of hidden strangeness in nucleons is thus an exciting possibility which may indicate the limits of that model. Hidden strangeness in the nucleon has been proposed recently on the basis of various experimental findings. Deep inelastic scattering reveals a significant $\bar{s}s$ contribution in the flavor wave function of the nucleon [1–3] but at large momentum transfers. The pion-nucleon sigma term $\Sigma_{\pi N}$ [4,5] derived from low-energy πN scattering also seems to require an $\bar{s}s$ component. However this interpretation is not undisputed [6,7].

The production of ϕ mesons is an alternative way to search for the strangeness content of the nucleon. ϕ mesons are dominantly $\bar{s}s$ and their production off protons may reflect an intrinsic hidden strangeness. Experiments on ϕ meson production in $\bar{p}p$ annihilation at rest into $\phi\ +X$ or $\omega\ +X$ show a strong violation of the OZI rule [8–10]. Particularly interesting is the high selectivity of the breakdown of the OZI rule: ϕ production is largely enhanced in some reactions but only slightly in others. However, conventional explanations of these findings also exist [11]–[14]. In particular the large rate for $\bar{p}p \to \phi\pi$ can be calculated from rescattering of the two kaons produced in $\bar{p}p \to K^*\bar{K}$. Note that the rates for these two reactions is similar in magnitude.

Another possibility to investigate the role of hidden strangeness in nucleons is offered by photoproduction of ϕ mesons off nucleons in the reaction

$$\gamma\ + p \to\ p + \phi; \quad \phi\ \to\ K^+K^- \qquad (1)$$

The $\phi\ \to\ K^+K^-$ is chosen because of its easy identification in a magnetic spectrometer. Due to the experimental possibilities offered by CEBAF and ELSA, this approach has attracted considerable interest.

Data on photoproduction of ϕ mesons are scarce so far. At Bonn, total and differential cross sections for reaction (1) were measured in the early '70ties [15]. The experiment used a spectrometer set and a fixed photon energy of 2 GeV. Data were taken at 5 different values of the momentum transfer. At higher energies ($2.8 < E_\gamma < 4.8$ GeV), low-statistics data are available from Daresbury [16] and DESY [17]. At Bonn, the SAPHIR Collaboration has collected more than 2000 ϕ mesons over a range of photon energies from the ϕ production threshold to 2.6 GeV. Two high-statistics experiments at CEBAF plan to investigate this reaction [18,19].

This renewed interest stems from a couple of new questions which concern the production mechanisms (see Fig. 1). The most prominent contribution to ϕ photoproduction comes from diffractive scattering which can be visualized as scattering of the ϕ component of the photon (through vector meson dominance) off the nucleon via Pomeron exchange. This can be seen from the dependence of cross section on the momentum transfer $t = t' - t'_{min}$ which falls off exponentially. The slope parameter is $\alpha \sim$-4 GeV^2; it depends weakly on energy. Other processes have not yet been established; pure pion exchange would give a stronger fall-off with t.

Figure 2 shows a recent calculation [24] for reaction (1) and a photon energy of 2 GeV. The different contributions are plotted and compared to the Bonn data [15]. Clearly, there is need to extend the data to backward ϕ production or large t.

The K^+K^- pair could also be produced with zero relative angular momentum. Indeed, experiments reported a

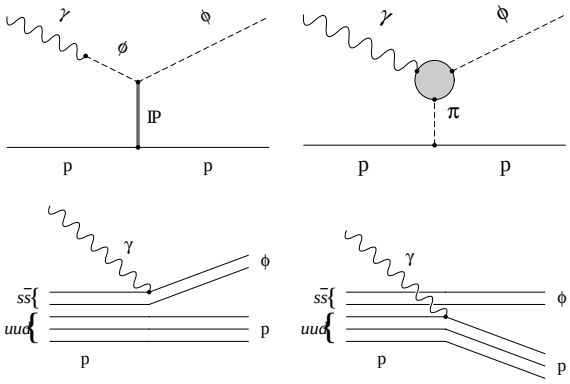

Fig. 1. Upper panel: ϕ-meson photoproduction via Pomeron exchange (left) and via pion exchange (right). Lower panel: ϕ-meson photoproduction via knockout of the hypothetical $\bar{s}s$ (left) and uud (right) component of the nucleon (from [24])

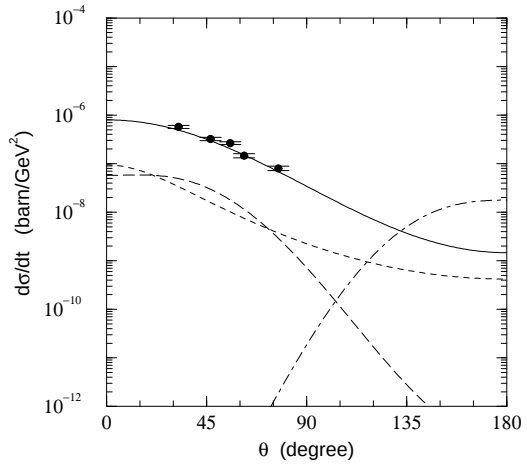

Fig. 2. Differencial cross section for ϕ meson photoproduction as a function of the scattering angle. The solid curve representing diffractive scattering describes the data very well. Deviations can occur at backward angles due to pion exchange (- - -) or due to knockout of the $\bar{s}s$ (– – –) or uud (- – -) component. The data are from Bonn [15], the calculation from Titov et al. [24]

$S-P$ interference effect [16]. The S wave part is particularly exciting since the photoproduction amplitude for production of scalar K^+K^- pairs may shed light on the internal structure of the $f_0(980)$ and $a_0(980)$ which is important in the present glueball discussion [20]. The second processes of the lower part of Fig. 1 are those of interest in the present discussion: the photon may be absorbed by the uud component and may give a kick into the forward direction. The $\bar{s}s$ may then be left behind, a ϕ is produced in backward direction.

In the next section we outline the derivation of the ϕ meson production due to rescattering mechanism. In Sect. 3 the diffractive ϕ meson production within the vector-meson-dominance model through the Pomeron exchange is discussed. In Sect. 4 a brief review of the helicity amplitudes and spin observables are given. The Sect. 5 the numerical results are presented.

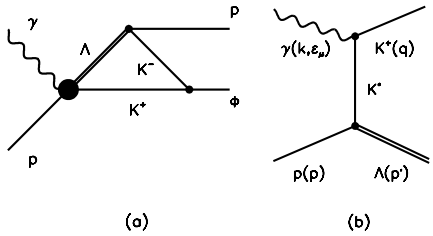

Fig. 3. **a** ϕ-meson photoproduction via rescattering with $\Lambda(1520)K^+$ production in the intermediate state; **b** photoproduction of $\Lambda(1520)$

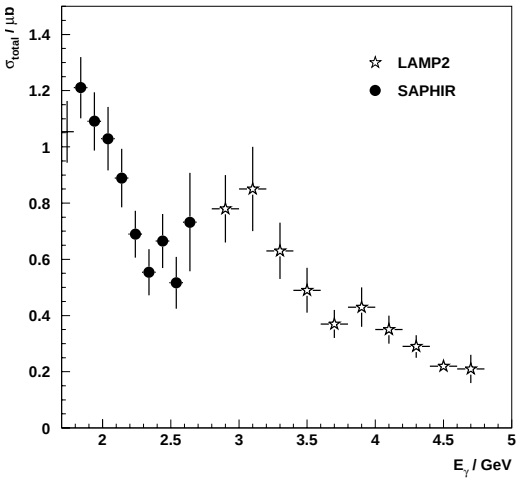

Fig. 4. Cross section for $\Lambda(1520)$ photoproduction. The data above 2.7 GeV are from Daresbury, the low-energy data are preliminary SAPHIR results. The threshold enhancement is associated with an angular distribution characteristic of a P_{13} resonance (from [25])

2 ϕ meson photoproduction via rescattering in dispersion technique

As mentioned, the search for an $s\bar{s}$-component in the nucleon and the hope for a better understanding of the nature of the $a_0(980)$ and $f_0(980)$ provide strong support for new experiments investigating ϕ-photoproduction. However, from ϕ production in $\bar{p}p$ annihilation we should have learned a lesson: rescattering effects can be important and its effects should be known in order to avoid a misinterpretation of the data. The final state pK^+K^- can be reached via ϕ photoproduction also via reaction

$$\gamma\ + p \to\ \Lambda(1520) + K^+; \qquad \Lambda(1520) \to pK^- \qquad (2)$$

where the $\Lambda(1520)$ decays with a fraction of 22% into pK^+ and the K^+ then rescatters with the K^- into a ϕ. The process is shown in Fig. 3a. The cross section for the photoproduction of $\Lambda(1520)$ is shown in Fig. 4. The low-energy part has been determined at by the SAPHIR collaboration [25], the results are still preliminary. The high energy data are from Daresbury [21]. The cross section is of similar magnitude as that for ϕ production. Hence kinematical ranges can exist in which rescattering of the two kaons may form a ϕ thus giving rise to a distortion of $\frac{d\sigma}{dt}$. This distortion

must be known, at least its order of magnitude, to prevent a misinterpretation of the data.

We calculate rescattering contributions to process (1) as two–step process: in a first step, the system $\Lambda(1520)\mathrm{K}^+$ is produced and then, after the decay of the $\Lambda(1520) \to p\mathrm{K}^-$, the $\overline{K}K$ system forms a ϕ–meson. This process is related to the three-meson dynamics in the intermediate state:

$$\gamma \ + p \to \ p\mathrm{K}^+\mathrm{K}^- \to \ p\phi \ . \tag{3}$$

2.1 A model for $\Lambda(1520)$ photoproduction: exchange of $K^*(890)$ meson Regge trajectories

In this model we assume that the $\Lambda(1520)$ in $\gamma p \to \Lambda(1520)$ K^+ is produced by the exchange of dominant meson Regge trajectories in the t-channel. The dominant meson trajectories are the K and $K^*(890)$. It was shown that the K^* gives the main contribution to the cross section at the energies $E_\gamma > 5$ GeV [23]. In our energy region $E_\gamma \sim 2$ GeV it is possible that not only t-channel exchanges but also s-channel resonances contribute to the $\Lambda(1520)$ photoproduction. Furthermore, at small t the contribution from K-exchange increases. Unfortunately the lack of experimental information about $\Lambda(1520)$ photoproduction does not allow to build a model which takes into account all contributions mentioned above. Therefore we use a simple model in our calculation where the K^* trajectory gives the main contribution into $\Lambda(1520)$ photoproduction. In this approach the unknown parameters of the model, the form factors, can be defined using the experimental cross section which effectively takes also into account the contribution from other t-channel exchanges. Let us denote the four-momenta of the incoming photon, outgoing kaon, initial proton and final Λ as k, q, p and p' respectively. The invariant amplitude for $\Lambda(1520)$ photoproduction (Fig. 3b) then can be written as

$$T_\Lambda = \epsilon^\gamma_\mu M_\mu T_0 \tag{4}$$

with

$$M_\mu = \bar{\Psi}_\nu(p') Q^{\mu\alpha}_{\gamma K^* K} Q^{\alpha\nu}_R u(p) \tag{5}$$

where ϵ^γ_μ is photon polarization vector, $u(p)$ is the Dirac spinor of the proton with momentum p and $\Psi_\nu(p')$ is spinor of the Λ. The vertex operator for $\gamma K^* K$, $Q^{\mu\alpha}_{\gamma K^* K}$, is given by

$$Q^{\mu\alpha}_{\gamma K^* K} = \epsilon_{\mu\alpha\beta\delta} k_\beta q_\delta \tag{6}$$

where $\epsilon_{\mu\alpha\beta\gamma}$ is the rank-4 antisymmetrical tensor. The vertex operator for $pK^*\Lambda$, $Q^{\alpha\nu}_R$, can be written as

$$Q^{\alpha\nu}_R = g_{\alpha\nu}(\hat{p'} - \hat{p}) - \gamma_\alpha(p'_\nu - p_\nu) \ . \tag{7}$$

This operator is orthogonal to the momentum of K^* which allows to perform a summation over α in (4) (the term proportional to $(p' - p)_\alpha$ in the K^* propagator could be omitted). The normalization parameter T_0 includes the vertex coupling constants, form factor and K^* trajectory. Let us note that T_0 is complex and its phase is due to the phase factor in Regge trajectory $1 + Sexp(-i\pi\alpha(t))$ where $S = -1$ is the signature of the K^* trajectory and $\alpha(t) = 0.25 + 0.83t$. The module of T_0 which depends on the invariant $t = (p' - p)^2$ and $s = (k + p)^2$ is defined by the cross section:

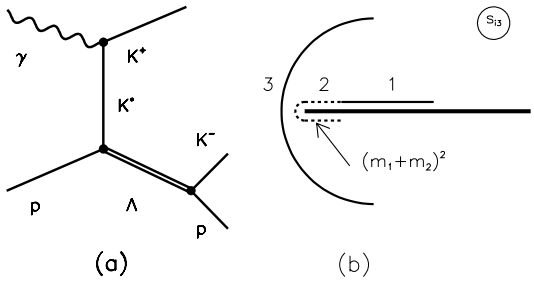

Fig. 5. a Photoproduction of $\Lambda(1520)$ and its decay into proton and kaon; **b** position of the integration contour $C(s'_{12})$

$$|\ T_0\ |^2 = \frac{16\pi(s - m_N^2)^2 \frac{d\sigma}{dt}}{Tr} \tag{8}$$

where Tr comes from the summation over final states and average over initial states:

$$Tr = \frac{1}{4} g_{\mu\mu'} Q^{\mu\alpha}_{\gamma K^* K} Q^{\mu'\alpha'}_{\gamma K^* K} Tr\Bigg\{ (\hat{p} + m) Q^{\alpha\nu}_R (\hat{p'} + m_\Lambda) \times \left(-g^\perp_{\nu\nu'} + \frac{1}{3}\gamma^\perp_\nu \gamma'^\perp_\nu \right) Q^{\alpha'\nu'}_R \Bigg\} \tag{9}$$

where we take into account the completeness condition for 3/2-spin spinors (62).

To write down the process for photoproduction of a $\Lambda(1520)$ which decays into pK^- one should use the decay matrix element (64). Again taking into account the completeness condition for 3/2-spin spinors (62) one finds that the amplitude for the reaction of Fig. 5a is equal to:

$$A_\Lambda = \epsilon^\gamma_\mu T_0 Q^{\mu\alpha}_{\gamma K^* K} Q^{\alpha\nu}_R \times \frac{\left(\hat{P'} + m_\Lambda\right)\left(-g^\perp_{\nu\beta} + \frac{1}{3}\gamma^\perp_\nu \gamma^\perp_\beta\right)}{m_\Lambda^2 - P'^2 - i m_\Lambda \Gamma} \gamma_5 k_{N\mu} g_{\Lambda NK} \tag{10}$$

where P' and k_N are momenta of the Λ and nucleon, respectively.

2.2 Rescattering with ϕ production in the final state

In this section it is shown how rescattering in the final state can be calculated in the framework of the dispersion relation technique. Let us consider the process of Fig. 3a where the ϕ in the final state is produced via rescattering with an $\Lambda(1520)$ in the intermediate state. Let us denote K^+, K^- and p as the first, the second and the third particles, respectively. The momenta of the K^+ and the K^- in the intermediate state are p'_1 and p'_2, respectively, and the momentum of the proton p_3. We will consider the general

case when all particles have different masses, m_1, m_2 and m_3.

Our aim is to write down the dispersion relation over invariant mass of particles 1 and 2 in the intermediate state. According to the general rules of the dispersion technique [34] we start from calculating the discontinuity of the triangle diagrams in the channel of particles 1 and 2:

$$disc T^{tr} \;=\; \frac{1}{2}\int d\Phi(KK)\; A_\Lambda Q_{\phi\to KK}\;. \qquad (11)$$

A_Λ defines the amplitude for $\Lambda(1520)$ photoproduction, $Q_{\phi\to KK}$ is the matrix element for ϕ decay into two kaons given by (46) and the $d\Phi(KK)$ is the phase space element given by (50). It is convenient to perform the phase space integration in (11) in the c.m. frame of particles 1 and 2. In this frame

$$\begin{aligned} s_{13} &= m_1^2 + m_3^2 - 2p'_{10}p_{30} + 2z_{13}\mathbf{p'_1}\mathbf{p_3};, \\ p'_{10} &= \frac{s'_{12}+m_1^2-m_2^2}{2\sqrt{s'_{12}}}\;, \qquad \mathbf{p'_1} = \sqrt{p'^2_{10}-m_1^2}, \\ P_{30} &= \frac{s'_{12}+m_3^2-s}{2\sqrt{s'_{12}}}\;, \qquad \mathbf{p_3} = \sqrt{p_{30}^2-m_3^2}, \end{aligned} \qquad (12)$$

where $z_{13}=\cos\theta_{13}$ and θ_{13} is the angle between the particles 1 in the intermediate state and 3 in the cms of particles 1 and 2, $s=(p_1+p_2+p_3)^2$, and $s'_{12}=(p'_1+p'_2)^2$. The expression for s_{23} is obtained from (12) by the replacement $1\leftrightarrow 2$. Equation (11) can be transformed to an integral over the solid angle:

$$disc T^{tr} \;=\; \frac{1}{2}\int \frac{d\Omega_{1'2'}}{4\pi}\; A_\Lambda Q_{\phi\to KK}\;\rho_{12}(s'_{12}) \qquad (13)$$

where

$$\begin{aligned} \rho_{12}(s'_{12}) &= \frac{1}{16\pi s'_{12}} \qquad (14)\\ &\times\sqrt{[s'_{12}-(m_1+m_2)^2][s'_{12}-(m_1-m_2)^2]}\;. \end{aligned}$$

To perform an integration over the solid angle we define the z-axis along the $\mathbf{p_3}$ vector. We also introduce the relative momentum of the particles 1 and 2, $k'=p'_1-p'_2$, with:

$$\begin{aligned} k'_x &= \mathbf{k}'\;\sin\theta_{13}\;\cos\phi, \quad k'_y \;=\; \mathbf{k}'\;\sin\theta_{13}\;\sin\phi, \\ k'_z &= \mathbf{k}'\;\cos\theta_{13} \qquad (15)\\ \mathbf{k}'^2 &= \frac{1}{s'_{12}}\;[s'_{12}-(m_1+m_2)^2][s'_{12}-(m_1-m_2)^2]\;. \qquad (16) \end{aligned}$$

ϕ is the azimuthal angle. As the next step we should decompose the vectors in (13) into an internal vector k' and external vectors p_3, k and p. Due to the integration over ϕ the terms proportional to k_α, $k_\alpha k_\beta k_\gamma$, $k_\alpha k_\beta k_\gamma k_\mu k_\nu$ will be equal to zero.

The integration over z has to be carried out along the contour $C(s'_{12})$ shown in Fig. 5b. As shown in [35] the integration contour $C(s'_{12})$ at small s'_{12},

$$\begin{aligned} &(m_1+m_2)^2 \le s'_{12} \le \frac{m_i s}{m_i+m_3} \\ &+\frac{m_3}{m_i+m_3}\;(m_1+m_2-m_i)^2 - m_i m_3 \equiv s_{i3}(R), \qquad (17) \end{aligned}$$

coincides with the phase space integration contour

$$-1 \le z_{i3} \le 1. \qquad (18)$$

shown in Fig. 5b by the solid line 1. At

$$s_{i3}(R) \le s'_{12} \le (\sqrt{s}-m_3)^2 \qquad (19)$$

the contour $C(s'_{12})$ contains an additional part (Fig. 5b, dashed line 2.) At $s'_{12} > (\sqrt{s}-M_3)^2$ the integration is performed in the complex s_{i3}-plane (line 3, Fig. 5b).

Finally, we find that the amplitude of the triangle diagram including the $\Lambda(1520)$ production in the intermediate state is given by the following dispersion integral:

$$T^{tr} \;=\; \int_{4M_K^2}^{\Lambda_{cut}} \frac{ds'_{12}}{\pi}\;\frac{disc(T^{tr})}{s'_{12}-s_{12}}\;. \qquad (20)$$

Here Λ_{cut} is a cutting parameter for the K^+K^- channel. The introduction of a cut-off in the dispersion integral ensures its convergence and should be interpreted as a compensation for our ignorance of the real K^+K^- amplitude at high energies. It is important to note that the diagrams which contain rescattering and include resonances in the intermediate state have an anomalous singularity which may appear near the physical region. These anomalous singularities are related to the processes going at large distances. At correct calculation of the rescattering process (independently of the technique used, either Feynman diagram or dispersion representation) these singularities are correctly taken into account. In the dispersion technique the correct account for singularities is related to the correct choice of the integration contour when $disc T^{tr}$ is calculated: the correct position of the integration contour is shown in Fig. 5b (for details see [35]).

3 ϕ photoproduction through Pomeron exchange

The photoproduction of the ϕ meson can be described in the framework of the vector-meson dominance model (VDM). In this model [26,27], the incoming photon first converts into a ϕ meson and then scatters diffractively from the nucleon through Pomeron exchange (see Fig. 1).

A microscopic model for vector-meson photo- and electro-production at high energy is based on the Pomeron–photon analogy [36]. The Pomeron was described successfully in terms of a non-perturbative two-gluon exchange model [28–33].

We will follow the [24] where the vector-meson dominance model with Pomeron-photon analogy within the hadron-Pomeron interaction picture is used, which is expected to be valid in the low energy region. In this approach, the incoming photon first converts into a quark and antiquark pair, which then exchanges a Pomeron with one of the quarks in the proton before it recombines into an outgoing ϕ meson. The invariant amplitude of the diffractive production can be written as

$$T^{\rm VDM} = iT_0\varepsilon^{*\phi}_\mu \mathcal{M}^{\mu\nu}\varepsilon^\gamma_\nu, \qquad (21)$$

with

$$\mathcal{M}^{\mu\nu} = O_\alpha \Gamma^{\alpha,\mu\nu}, \tag{22}$$

where O_α describes the Pomeron-nucleon vertex and $\Gamma^{\alpha,\mu\nu}$ is associated with the Pomeron–vector-meson coupling which is related to the $\gamma \to q\bar{q}$ vertex Γ_ν and the $q\bar{q} \to \phi$ vertex V_μ, as shown in Fig. 11. The dynamics of the Pomeron-hadron interactions is contained in T_0. The Pomeron-nucleon vertex is given by

$$O_\alpha = \bar{u}(p')\gamma_\alpha u(p). \tag{23}$$

It is derived in [24] that in the case of ϕ meson photoproduction the Pomeron-vector-meson vertex can be written as

$$\tilde{\Gamma}^{\alpha,\mu\nu} = (k+q)^\alpha g^{\mu\nu} - 2k^\mu g^{\alpha\nu}, \tag{24}$$

The factor T_0 in (21) can be defined from the dynamics of the Pomeron-hadron interaction. We use the parametrisation of the differential cross section determined in [37]:

$$\left(\frac{d\sigma}{dt}\right)_{\rm VDM} = \sigma b \exp(-b|t - t_{\max}|), \tag{25}$$

with $b = 4.01$ GeV^{-2} and $\sigma = 0.2$ μb. Then normalization factor T_0 can be found from (8) where square of the amplitude is given by

$$Tr = \frac{1}{4} g_{\nu\nu'} \left(g_{\mu\mu'} - \frac{q_\mu q'_\mu}{q^2}\right) \times Tr\left\{(\hat{p}+m)\tilde{\Gamma}^{\alpha,\mu\nu}\gamma_\alpha(\hat{p'}+m)\tilde{\Gamma}^{\alpha',\mu'\nu'}\gamma'_\alpha\right\}. \tag{26}$$

Let us stress that in our approach we consider the pomeron as a phenomenological object for the description of a t-channel exchange by vacuum quantum numbers, that leads to the diffractive scattering. The parameter α'_P of this "low-energy pomeron" is close to zero, for the diffractive cone slope of the elastic scattering it is almost constant (the shrinkage of the diffractive cone becomes noticeable at higher energies only). If there is no shrinkage, the growth of the real part of the amplitude with $|t|$ is also suppressed and can be neglected.

4 Helicity amplitudes and spin observables

In this section a brief review on helicity amplitudes and on the definition of the different polarization observables is given. Details of this formalism can be found in [38–42].

To study spin observables, it is useful to use helicity amplitudes in the c.m. frame:

$$H_{\lambda_\phi,\lambda_f;\lambda_\gamma,\lambda_i} \equiv \langle \mathbf{q};\lambda_\phi,\lambda_f\,|\,T\,|\,\mathbf{k};\lambda_\gamma,\lambda_i\rangle, \tag{27}$$

where $\mathbf{k}$ and $\mathbf{q}$ are the momenta of the initial and final system, respectively. λ_γ $(=\pm1)$, λ_ϕ $(=0,\pm1)$ and $\lambda_{i,f}$ $(=\pm1/2)$ are the helicities of the photon, ϕ meson and target proton or recoil proton. In principle, there are $2\times 2\times 3\times 2 = 24$ complex amplitudes. However, due to the parity invariance relation,

$$\langle \mathbf{q};\lambda_\phi,\lambda_f|\,T\,|\mathbf{k};\lambda_\gamma,\lambda_i\rangle = (-1)^{\Lambda_f-\Lambda_i}\langle \mathbf{q};-\lambda_\phi,-\lambda_f\,|\,T\,|\,\mathbf{k};-\lambda_\gamma,-\lambda_i\rangle, \tag{28}$$

with $\Lambda_f = \lambda_\phi - \lambda_f$ and $\Lambda_i = \lambda_\gamma - \lambda_i$, only 12 complex helicity amplitudes are independent. We label them as in [41]:

$$\begin{aligned}
H_{1,\lambda_\phi} &\equiv \langle \lambda_\phi,\, \lambda_f = +\tfrac{1}{2}\,|\,T\,|\,\lambda_\gamma = 1,\, \lambda_i = -\tfrac{1}{2}\rangle,\\
H_{2,\lambda_\phi} &\equiv \langle \lambda_\phi,\, \lambda_f = +\tfrac{1}{2}\,|\,T\,|\,\lambda_\gamma = 1,\, \lambda_i = +\tfrac{1}{2}\rangle,\\
H_{3,\lambda_\phi} &\equiv \langle \lambda_\phi,\, \lambda_f = -\tfrac{1}{2}\,|\,T\,|\,\lambda_\gamma = 1,\, \lambda_i = -\tfrac{1}{2}\rangle,\\
H_{4,\lambda_\phi} &\equiv \langle \lambda_\phi,\, \lambda_f = -\tfrac{1}{2}\,|\,T\,|\,\lambda_\gamma = 1,\, \lambda_i = +\tfrac{1}{2}\rangle.
\end{aligned} \tag{29}$$

The ϕ-meson photoproduction amplitude can then be represented by a 6×4 matrix $\mathcal{F}$ in helicity space;

$$\mathcal{F} \equiv \begin{pmatrix}
H_{2,1} & H_{1,1} & H_{3,-1} & -H_{4,-1}\\
H_{4,1} & H_{3,1} & -H_{1,-1} & H_{2,-1}\\
H_{2,0} & H_{1,0} & -H_{3,0} & H_{4,0}\\
H_{4,0} & H_{3,0} & H_{1,0} & -H_{2,0}\\
H_{2,-1} & H_{1,-1} & H_{3,1} & -H_{4,1}\\
H_{4,-1} & H_{3,-1} & -H_{1,1} & H_{2,1}
\end{pmatrix}. \tag{30}$$

In the previous sections we have calculated the matrix elements of the amplitude in the nucleon spin space. They are related to the helicity amplitude discussed above by

$$H_{\lambda_\phi,\lambda_f;\lambda_\gamma,\lambda_i} = (-1)^{1-\lambda_i-\lambda_f}\sum_{m_i,m_f} \times d^{(1/2)}_{m_i,-\lambda_i}(0)\, d^{(1/2)}_{m_f,-\lambda_f}(\theta)\langle \lambda_\phi, m_f\,|\,T\,|\,\lambda_\gamma, m_i\rangle. \tag{31}$$

The matrix $\mathcal{F}$ allows us to derive the different observables. For example, the unpolarized differential cross section:

$$\frac{d\sigma}{d\Omega}^{(U)} = \frac{\rho_0}{4}\,{\rm Tr}\,(\mathcal{F}\mathcal{F}^\dagger) \equiv \rho_0 \mathcal{I}(\theta), \tag{32}$$

where $\mathcal{I}(\theta)$ is the cross section intensity and $\rho_0 = |\mathbf{q}|/(\mathbf{64}\pi^{\mathbf{2}}\mathbf{s}|\mathbf{k}|)$.

If the incoming photon beam is polarized, one can define the polarized beam asymmetry (analyzing power) Σ_x as

$$\Sigma_x = \frac{{\rm Tr}\,[\mathcal{F}\sigma^x_\gamma \mathcal{F}^\dagger]}{{\rm Tr}\,(\mathcal{F}\mathcal{F}^\dagger)}. \tag{33}$$

If the cross section is given by $\sigma^{(B,T;R,V)}$ – the superscripts $(B,T;R,V)$ denote the polarizations of (photon beam, target proton; recoil proton, produced vector-meson) –, the physical meaning of Σ_x is:

$$\Sigma_x = \frac{\sigma^{(\|,U;U,U)} - \sigma^{(\perp,U;U,U)}}{\sigma^{(\|,U;U,U)} + \sigma^{(\perp,U;U,U)}}, \tag{34}$$

The superscript U refers to an unpolarized particle and $\|$ $(\perp)$ corresponds to a photon linearly polarized along the $\hat{\mathbf{x}}$ $(\hat{\mathbf{y}})$ axis.

In the same way the polarized target asymmetry T, recoil polarization asymmetry P, and the vector-meson polarization asymmetry V can be defined:

$$T_y = \frac{\mathrm{Tr}\,(\mathcal{F}\sigma_N^y\mathcal{F}^\dagger)}{\mathrm{Tr}\,\mathcal{F}\mathcal{F}^\dagger)}, \quad P_{y'} = \frac{\mathrm{Tr}\,(\mathcal{F}\mathcal{F}^\dagger\sigma_{N'}^{y'})}{\mathrm{Tr}\,(\mathcal{F}\mathcal{F}^\dagger)}. \tag{35}$$

$$V_j = \frac{\mathrm{Tr}\,(\mathcal{F}\mathcal{F}^\dagger\Omega_j^V)}{\mathrm{Tr}\,(\mathcal{F}\mathcal{F}^\dagger)}, \tag{36}$$

The physical meaning of T_y and $P_{y'}$ is:

$$T_y = \frac{\sigma^{(U,+y;U,U)} - \sigma^{(U,-y;U,U)}}{\sigma^{(U,+y;U,U)} + \sigma^{(U,-y;U,U)}}, \tag{37}$$

$$P_{y'} = \frac{\sigma^{(U,U;y',U)} - \sigma^{(U,U;-y',U)}}{\sigma^{(U,U;y',U)} + \sigma^{(U,U;-y',U)}}, \tag{38}$$

where the superscripts $\pm y$ and $\pm y'$ denote the direction of the target and recoil polarization respectively.

The six double polarization observables, Beam–Target (BT), Beam–Recoil (BR), Target–Recoil (TR), Beam–Vector-meson (BV), Target–Vector-meson (TV), and Recoil–Vector-meson (RV), can be defined as:

$$C_{ij}^{\mathrm{BT}} = \frac{\mathrm{Tr}\,[\mathcal{F}\sigma_\gamma^i\sigma_N^j\mathcal{F}^\dagger]}{\mathrm{Tr}\,(\mathcal{F}\mathcal{F}^\dagger)}, \tag{39}$$

$$C_{ij}^{\mathrm{BR}} = \frac{\mathrm{Tr}\,[\mathcal{F}\sigma_\gamma^i\mathcal{F}^\dagger\sigma_{N'}^j]}{\mathrm{Tr}\,(\mathcal{F}\mathcal{F}^\dagger)}, \tag{40}$$

$$C_{ij}^{\mathrm{TR}} = \frac{\mathrm{Tr}\,[\mathcal{F}\sigma_N^i\mathcal{F}^\dagger\sigma_{N'}^j]}{\mathrm{Tr}\,(\mathcal{F}\mathcal{F}^\dagger)}, \tag{41}$$

$$C_{ij}^{\mathrm{BV}} = \frac{\mathrm{Tr}\,[\mathcal{F}\sigma_\gamma^i\mathcal{F}^\dagger\Omega_j^V]}{\mathrm{Tr}\,(\mathcal{F}\mathcal{F}^\dagger)}, \tag{42}$$

$$C_{ij}^{\mathrm{TV}} = \frac{\mathrm{Tr}\,[\mathcal{F}\sigma_N^i\mathcal{F}^\dagger\Omega_j^V]}{\mathrm{Tr}\,(\mathcal{F}\mathcal{F}^\dagger)}, \tag{43}$$

$$C_{ij}^{\mathrm{RV}} = \frac{\mathrm{Tr}\,[\mathcal{F}\mathcal{F}^\dagger\sigma_{N'}^i\Omega_j^V]}{\mathrm{Tr}\,(\mathcal{F}\mathcal{F}^\dagger)}, \tag{44}$$

The physical meaning of e.g. C_{zz}^{BT} is then

$$C_{zz}^{\mathrm{BT}} = \frac{\mathrm{Tr}\,[\mathcal{F}\sigma_\gamma^z\sigma_N^z\mathcal{F}^\dagger]}{\mathrm{Tr}\,(\mathcal{F}\mathcal{F}^\dagger)} = \frac{\sigma^{(r,z;U,U)} - \sigma^{(r,-z;U,U)}}{\sigma^{(r,z;U,U)} + \sigma^{(r,-z;U,U)}}, \tag{45}$$

where the superscript r corresponds to a circularly polarized photon beam with helicity $+1$, and $\pm z$ denotes the direction of the target proton polarization (see [24] for explicit definition of double polarization observables).

5 Numerical results

In this section the results of our calculation for the unpolarized cross section and for single and double polarization observables are presented. The rescattering process is the two–step process: (1) production of $\Lambda(1520)\mathrm{K}^+$ system and (2) the decay of the $\Lambda(1520) \to p\mathrm{K}^-$ and forming a ϕ–meson. The second (rescattering) process has been calculated using the dispersion technique while the information about $\Lambda(1520)\mathrm{K}^+$ production is extracted from experimental data.

The differential cross section for $\Lambda(1520)$ photoproduction is not well known in the region of 2 GeV. The region of higher energies was investigated in [16] where the differential cross section was averaged over the incident photon energy from 2.8 to 4.8 GeV. The data show a strong diffractive peak, the differential cross section was parametrised as $exp(6.1 \pm 2.0)t$. The preliminary data for $\Lambda(1520)$ photoproduction at 2 GeV from SAPHIR [25] also show a forward diffractive peak but it is not so sharp and so even a linear behavior of the differential cross section could be assumed which falls to zero in the backward scattering region. In the calculation both variants have been investigated. We also assume that the total cross section for the $\Lambda(1520)$ photoproduction is equal to $1\mu b$ according to the preliminary data from [25].

Another source of uncertainties comes from the fact that the short-range behavior of the meson-meson and nucleon-meson interactions is unknown. It leads to the introduction of a cut-off Λ_{cut} in the dispersion integral which ensures its convergence. It should be interpreted as a compensation of our ignorance of the amplitude at higher energies. Let us discuss the vertex $K\bar{K} \to \phi$ in detail. If the ϕ meson would be a composite $K\bar{K}$ system, one would have the wave function of ϕ meson in the dispersion integral, and the integration region over s'_{12} in (20) would be defined by the area where the wave function is not small (the method of going from vertex function to wave function for the dispersion integral of such a kind was discussed in details in [34] using deuteron as example). But the ϕ-meson is, according to the quark model, the $s\bar{s}$ system, and in the hadron language the $K\bar{K}$ is only one possible component of the ϕ-meson. Let us assume that the $\phi \to K\bar{K}$ vertex is not small in the region where the vertex $\phi \to s\bar{s}$ also not small. The ϕ-meson wave function is well-known in the quark model: using the variable s'_{12} it can be approximated as $exp(-bs'_{12})$ with $b \simeq 2$ GeV^{-2} (for a detailed discussion of the ϕ-meson wave function see [43]). Then in the integral (20) the significant integration region is of the order of 1/b, that gives $\Lambda_{cut} - 4m_K^2 \sim 1/b \simeq 0.5$ GeV^2 or $\Lambda_{cut} = 1.5$ GeV^2: that was used in one of our estimations. Actually one may believe that the transition form factor $\phi \to K\bar{K}$ decreases more rapidly than the vertex $\phi \to s\bar{s}$ because the $K\bar{K}$ system consists of four quarks, and the integration region in (20) is effectively smaller. So, the value $1/b$ does determine a natural hadronic scale. The use of the arbitrary parameter Λ_{cut} in the range 1 – 2 GeV in our evaluations responds to our formulation of the problem: we evaluate the order of effects from various peripheral processes.

Figure 6a demonstrates the dependence of the unpolarized cross section on the assumption made for the differential cross section of $\Lambda(1520)$ photoproduction. The results for an exponential and a linear differential cross

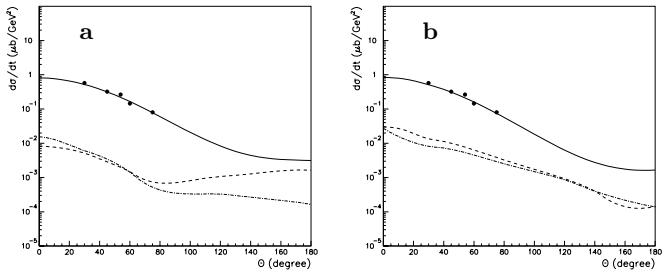

Fig. 6a,b. Cross section $\frac{d\sigma}{dt}$ for ϕ meson photoproduction as a function of the scattering angle. The solid curve represents diffractive scattering due to Pomeron exchange. **a** The dashed and dot-dashed line gives the contribution from rescattering in case of exponential and linear differential cross section for $\Lambda(1520)$ photoproduction. **b** The dashed and dot-dashed line give the contribution from rescattering with $\Lambda_{cut} = 1.5$ GeV^2 and $\Lambda_{cut} = 2$ GeV^2, respectively

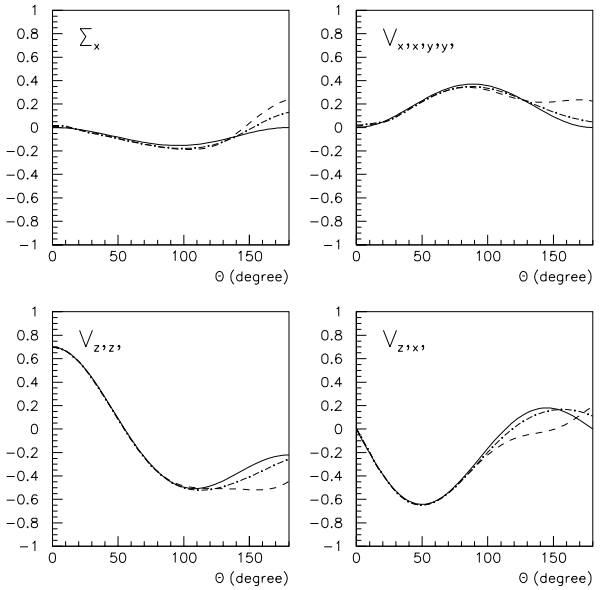

Fig. 7. Single spin observables. The solid curve represents diffractive scattering due to Pomeron exchange. The dashed and dot-dashed line give the contribution from Pomeron exchange+rescattering in case of exponential and linear differential cross section for $\Lambda(1520)$ photoproduction

section is given. For simplicity only the principle part of the dispersion integral is taken into account. Calculations using different cutting parameters, $\Lambda_{cut} = 1.5$ GeV^2 and $\Lambda_{cut} = 2$ GeV^2 in case the exponential cross section for $\Lambda(1520)$ photoproduction are shown in Fig. 6b.

The contribution of the rescattering process to the cross section has the same order of magnitude than other non-dominant contributions like e.g. pion exchange, (see Fig. 2). Nevertheless it is small compared to the dominant Pomeron exchange process. Therefore we do not expect a high sensitivity of unpolarised measurements on the contribution due to rescattering.

The situation is quite different in the measurement of single and double polarization observables. In Figs. 7 and 8 the results of the calculations for single and double spin

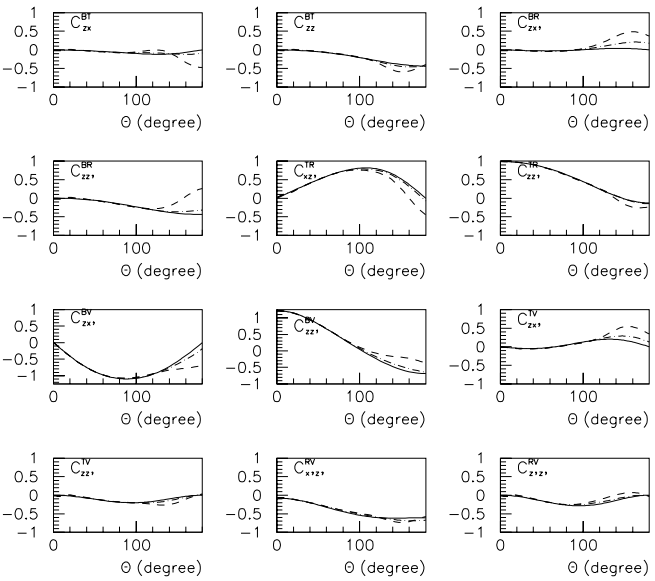

Fig. 8. Double spin observables. The solid curve represents diffractive scattering due to Pomeron exchange. The dashed and dot-dashed line give the contribution from Pomeron exchange+rescattering in case of exponential and linear differential cross section for $\Lambda(1520)$ photoproduction

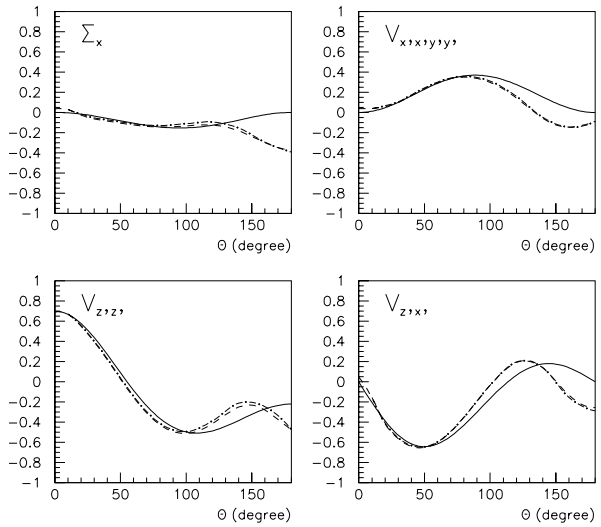

Fig. 9. Single spin observables. The solid curve represents diffractive scattering due to Pomeron exchange. The dashed and dot-dashed line give the contribution from Pomeron exchange+rescattering with Λ_{cut} equal to 1.5 and 2 GeV^2 respectively

observables are shown using different assumptions for the $\Lambda(1520)$ photoproduction cross section. Similar calculations with different cutting parameters, $\Lambda_{cut} = 1.5$ GeV^2 and $\Lambda_{cut} = 2$ GeV^2 for an exponential $\Lambda(1520)$ photoproduction cross section are shown in Figs. 9 and 10.

These results show that rescattering does not affect the polarization observables in the forward scattering region in comparison with Pomeron exchange. In [24] it was found that some double polarization observables in the forward scattering region, notably, $C^{\rm BT}_{zx,zz}$, $C^{\rm BR}_{zx',zz'}$,

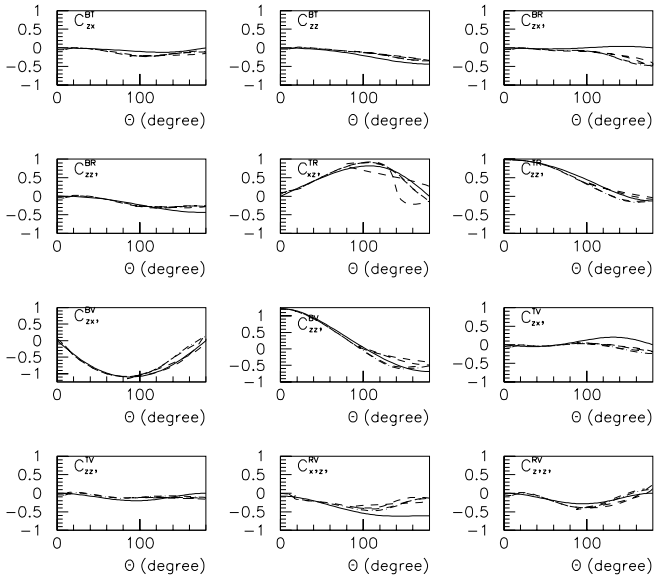

Fig. 10. Double spin observables. The solid curve represents diffractive scattering due to Pomeron exchange. The dashed and dot-dashed line give the contribution from Pomeron exchange+rescattering with Λ_{cut} equal to 1.5 and 2 GeV^2 respectively

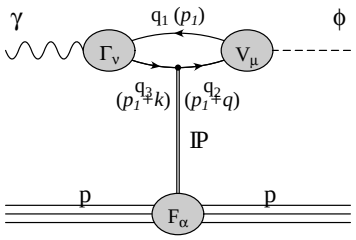

Fig. 11. Quark picture for the Pomeron exchange model of ϕ photoproduction (from [24]). The four-momenta of the quarks $q_{1,2,3}$ are given in parentheses

$C^{\rm TV}_{zx',zz'}$, and $C^{\rm RV}_{xx',zz'}$, depend very sensitively on the hidden strangeness content of the proton. Our calculations show that rescattering gives a visible effect on single and double polarization observables but only in the scattering region of $\theta \geq 90°$. This is the main difference between the contribution from rescattering and from the $s\bar{s}$-knockout mechanism in ϕ photoproduction. The large contribution from rescattering could be observed by measuring single polarization observables. They have the same order of magnitude as the $s\bar{s}$-knockout but a different angular dependence (see Fig. 9 from [24]). To distinguish between rescattering and $s\bar{s}$-knockout mechanism more information about $\Lambda(1520)$ photoproduction cross section is needed to decrease the uncertainties of rescattering calculation.

6 Conclusion

Photoproduction of ϕ mesons gives us the possibility to investigate the role of hidden strangeness in nucleons. The interpretation of the experimental data and any conclusion about the $\bar{s}s$ component in the proton wave function should however take into account possible conventional explanations. We investigated the production of hidden strangeness in the peripheral processes, which can be reliably evaluated using hadron language. Our investigation points out problems which can arise if one tries to determine the role of the hidden $s\bar{s}$ component in photon-proton reactions. Ignoring rescattering effects may lead to a wrong interpretation of the data.

We calculate the contribution from rescattering of K^+K^- pairs produced by photoproduction of $\Lambda(1520)K^+$ to photoproduction of ϕ mesons. We find that rescattering makes an important contribution to the photoproduction of ϕ mesons in the backward region ($\theta \geq 90°$) visible in the single and double polarization observables. Forthcoming high precision data may decide on the validity of the different models.

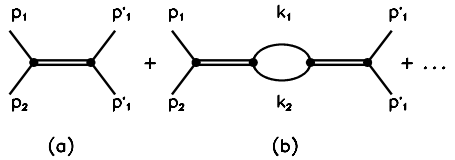

Fig. 12a,b. Series of diagrams for the resonance amplitude

Acknowledgements. We acknowledge the support from the Deutsche Forschungsgemeinschaft (436 RUS 17/98/99) and want to thank E. Klempt for illuminating discussions.

A Decay matrix elements and the coupling constant

A.1 $\phi \to KK$

The matrix element for the ϕ decay into two kaons is proportional to the relative momentum and can be written as

$$Q_{\phi\to KK} = \epsilon^{\phi}_{\mu}(p_1 - p_2)_{\mu} g_{\phi KK} \tag{46}$$

where $g_{\phi KK}$ is a coupling constant and p_i is the momentum of the kaon ($p_i^2 = m_K^2$). The completeness condition for the polarization vector ϵ^{ϕ} is

$$\epsilon^{\phi}_{\alpha}\epsilon^{\phi *}_{\beta} \;=\; -g^{\perp}_{\alpha\beta}(P)\;,$$

with

$$g^{\perp}_{\alpha\beta}(P) \;=\; g_{\alpha\beta} - \frac{P_\alpha P_\beta}{P^2}\;, \quad P \;=\; p_1 + p_2\;.$$

Here $g_{\mu\nu} = diag(1,-1,-1,-1)$. Now we consider the expression for a P-wave resonance in the framework of the dispersion technique which allows us to relate the coupling constant $g_{\phi KK}$ to the resonance width Γ. The amplitude for a P-wave resonance, a_R, can be presented as a series

of diagrams shown in Fig. 12. The first term in this series Fig. 12a is equal to

$$(p_1-p_2)_\mu\, g_{\phi KK}\, \frac{-g^\perp_{\mu\nu}(P)}{M^2-s}\, g_{\phi KK}\, (p'_1-p'_2)_\nu\,, \quad (47)$$

where $s=(p_1+p_2)^2$ and M is the mass of the bare resonance. The next term shown in Fig. 12b is equal to

$$(p_1-p_2)_\mu\, g_{\phi KK}\, \frac{-g^\perp_{\mu\mu'}(P)}{M^2-s} \times B_{\mu'\nu'}(s)\, \frac{-g^\perp_{\nu'\nu}(P)}{M^2-s}\, (p'_1-p'_2)_\mu\, g_{\phi KK}\,, \quad (48)$$

where $B_{\mu'\nu'}(s)$ is the amplitude of the loop diagram. Let us introduce the total momentum of the loop, $P'=k_1+k_2$, where $P'^2=s'$. To write down the dispersion integral for this diagram one should extract the invariant amplitude which depends on s' only. The imaginary part of the loop diagram is

$$\frac{1}{2}\int d\Phi(KK)\, (k_1-k_2)_{\mu'}\, g_{\phi KK}\, (k_1-k_2)_{\nu'}\, g_{\phi KK} \quad (49)$$

where the phase space element $d\Phi(KK)$ is

$$d\Phi(KK)=\frac{d^4k_1\, d^4k_2}{(2\pi)^6}\,(2\pi)^4\,\delta^4(P'-k_1-k_2) \times \delta(m_K^2-k_1^2)\,\delta(m_K^2-k_2^2)\,. \quad (50)$$

After integration over phase space, $d\Phi(KK)$, and the extraction of the tensor factor we find

$$B_{\mu'\nu'}(s)=-g^\perp_{\mu'\nu'}(P)\, b(s)\,. \quad (51)$$

The dispersion integral for $b(s)$ is

$$b(s)=\int\frac{ds'}{\pi}\,\frac{\frac{1}{3}\alpha(s')\rho(s')\, g^2_{\phi KK}}{s'-s}\,, \quad (52)$$

with

$$\rho(s')\equiv\frac{1}{2}\int d\Phi(KK)\;=\;\frac{1}{16\pi\sqrt{s'}}\,\sqrt{s'-4m_K^2}$$
$$\alpha(s')=s'-4m_K^2\,. \quad (53)$$

Thus, using the relation, $g^\perp_{\mu\mu''}(P)g^\perp_{\mu''\mu'}(P)\;=\;g^\perp_{\mu\mu'}(P)$ we find from (48) that diagram of Fig. 2b is equal to

$$-g^\perp_{\mu\nu}(P)\,(p_1-p_2)_\mu\, g_{\phi KK}\,\frac{1}{M^2-s} \times b(s)\,\frac{1}{M^2-s}\,(p_1-p_2)_\nu\, g_{\phi KK}\,. \quad (54)$$

Collecting terms with higher number of rescattering processes one finds that the amplitude of the ϕ which decays into two kaons is given by

$$a_R=(p_1-p_2)_\mu\, g_{\phi KK}\,\frac{-g^\perp_{\mu\nu}(P)}{M^2-s-b(s)}\,(p_1-p_2)_\nu\, g_{\phi KK}\,. \quad (55)$$

The standard Breit-Wigner formula can be obtained from (55) if one neglects the energy dependence in $b(s)$:

$$a_R=(p_1-p_2)_\mu\, g_{\phi KK}\,\frac{-g^\perp_{\mu\nu}(P)}{M_0^2-s-i\Gamma_0 M_0}\,(p_1-p_2)_\nu\, g_{\phi KK} \quad (56)$$

with

$$M_0^2=M^2-Re\; b(M_0^2), \quad (57)$$
$$\Gamma_0 M_0=\frac{1}{3}\alpha(M_0^2)\rho(M_0^2)g^2_{\phi KK}\,. \quad (58)$$

M_0 and Γ_0 are the physical mass and width of the resonance. Equation (58) defines g_1:

$$g^2_{\phi KK}\;=\;\frac{3\;\Gamma_0\;M_0}{\alpha(M_0^2)\rho(M_0^2)}\,. \quad (59)$$

A more sophisticated Breit-Wigner formula which takes into account two-particle thresholds can be obtained from (55), by neglecting the energy dependence in $Re\; b(s)$ only taking into account the threshold singularity:

$$\Gamma(s)=\;\Gamma_0\left(\frac{s-4m_K^2}{M_0^2-4m_K^2}\right)^{\frac{3}{2}} \quad (60)$$

A.2 $\Lambda(1520)\to pK^-$

Let us consider the matrix element for the decay $\Lambda(1520)$ into p and K^-. The $\Lambda(1520)$ is defined by the field $\Psi(P)$ which satisfies the conditions

$$P_\mu\,\Psi_\mu(P)\;=0\,,\quad \gamma_\mu\,\Psi_\mu(P)\;=0 \quad (61)$$

where P is the 4-momentum of the $\Lambda(1520)$. The completeness condition for 3/2-spin field can be written as:

$$\sum_a \Psi_{\mu a}(P)\bar\Psi_{\nu a}(P) = \left(\hat P+m_\Lambda\right)\left(-g^\perp_{\mu\nu}(P)+\frac{1}{3}\gamma^\perp_\mu(P)\gamma^\perp_\nu(P)\right) \quad (62)$$

with

$$g^\perp_{\mu\nu}(P)\;=g_{\mu\nu}-\frac{P_\mu P_\nu}{P^2}\,,\gamma^\perp_\mu(P)\;=\gamma_\mu-P_\mu\frac{\hat P}{P^2}\,. \quad (63)$$

The decay matrix element for the $\Lambda(1520)$ decay into nucleon and kaon has the form [22]:

$$Q_{\Lambda\to NK}=\Psi^\mu\,\gamma_5 k_{N\mu} g_{\Lambda NK} \quad (64)$$

where $g_{\Lambda NK}$ is a coupling constant and k_N is momentum of the nucleon.

Let us define the coupling constant for $\Lambda\to NK$, which determines the process of Fig. 5a. The propagator of the stable Λ, with mass m_Λ, is equal to

$$\frac{(\hat P+m_\Lambda)(-g^\perp_{\alpha\beta}+\frac{1}{3}\gamma^\perp_\alpha\gamma^\perp_\beta)}{m_\Lambda^2-P^2}\,. \quad (65)$$

The propagator in case of a decay into nucleon and kaon can be redefined by the replacement:

$$(m_\Lambda^2 - P^2)^{-1} \to (m_\Lambda^2 - P^2 - B_{NK}(P^2))^{-1}\,, \qquad (66)$$

where $B_{NK}(P^2)$ is the kaon–nucleon loop diagram. The real part of this diagram re-determines m_Λ, and the imaginary part of $B_{NK}(P^2)$ gives the partial width Γ for the decay $\Lambda \to KN$:

$$\frac{(\hat P + m_\Lambda)(-g^\perp_{\alpha\beta} + \frac{1}{3}\gamma^\perp_\alpha\gamma^\perp_\beta)}{m_\Lambda^2 - P^2 - i m_\Lambda \Gamma}\,. \qquad (67)$$

The next step is to calculate $B_{NK}(P^2)$. The following expression stands for the Λ propagator with $B_{NK}(P^2)$ considered as a perturbative correction:

$$\begin{aligned}&\frac{(\hat P + m_\Lambda)(-g^\perp_{\alpha'\beta} + \frac{1}{3}\gamma^\perp_{\alpha'}\gamma^\perp_\beta)}{m_\Lambda^2 - P^2}\\ &\times \int \frac{d^4k_N}{(2\pi)^4 i}\, k_{N\beta}\gamma_5\, \frac{(\hat k_N + m_N)}{m_N^2 - k_N^2}\,(-k_{N\alpha}\gamma_5)\,\frac{1}{m_K^2 - m_K^2}\\ &\times \frac{(\hat P + m_\Lambda)(-g^\perp_{\alpha\beta'} + \frac{1}{3}\gamma^\perp_\alpha\gamma^\perp_{\beta'})}{m_\Lambda^2 - P^2}\,. \qquad (68)\end{aligned}$$

Let us stress that in (68) one has a different sign for left and right operator to make the B-function positive.

Let us decompose the vector k_N over vectors P and $k^\perp$ ($k^\perp$ is orthogonal to p):

$$k_N = \frac{P^2 + m_N^2 - m_K^2}{2P^2}\; P + k^\perp\,. \qquad (69)$$

To calculate the imaginary part of (68) the following replacement should be made:

$$\begin{aligned}&\frac{1}{(m_K^2 - k_K^2)(m_N^2 - k_N^2)} \to\\ &\quad \frac{1}{2}(2\pi i)^2 \delta(m_N^2 - k_N^2)\theta(k_{N0})\delta(m_K^2 - k_K^2)\theta(k_{K0})\,. \qquad (70)\end{aligned}$$

When integrating over $k^\perp$, the terms proportional to $k^\perp$ and $k^{\perp 3}$ vanish, while the quadratic terms should be replaced as follows:

$$\begin{aligned}k^\perp_\alpha k^\perp_\beta &\to -\frac{1}{3}\left[m_K^2 - \frac{(P^2 - m_N^2 + m_K^2)}{4P^2}\right] g^\perp_{\alpha\beta}\\ &= -\frac{1}{3}k_\perp^2 g^\perp_{\alpha\beta}\,. \qquad (71)\end{aligned}$$

Using the equality

$$\left(g^\perp_{\alpha\beta} - \frac{1}{3}\gamma^\perp_\alpha\gamma^\perp_\beta\right)\left(g^\perp_{\beta\varepsilon} - \frac{1}{3}\gamma^\perp_\beta\gamma^\perp_\varepsilon\right) = \left(g^\perp_{\alpha\varepsilon} - \frac{1}{3}\gamma^\perp_\alpha\gamma^\perp_\varepsilon\right)\,. \qquad (72)$$

one obtains:

$$\begin{aligned}&\frac{\left(\hat P + m_\Lambda\right)\left(-g^\perp_{\alpha'\beta'} + \frac{1}{3}\gamma^\perp_{\alpha'}\gamma^\perp_{\beta'}\right)}{m_\Lambda^2 - P^2}\; i\frac{g^2_{\Lambda NK}}{24\pi}\\ &\times\left(\frac{(P^2 + m_N^2 - m_K^2)^2}{4P^2} - m_K^2\right)^{3/2}\\ &\times\frac{(m_\Lambda - m_N)^2 - m_K^2}{m_\Lambda}\,. \qquad (73)\end{aligned}$$

So

$$g^2_{\Lambda NK} = \frac{24\pi\Gamma m_\Lambda^2}{|\mathbf{k}|^3\left((m_\Lambda - m_N)^2 - m_K^2\right)} \qquad (74)$$

where $|\mathbf{k}|$ is the kaon momentum in the c.m. frame.

References

1. J. Ashman et al., Nucl. Phys. **B328** (1989) 1
2. D. Adams et al., Phys. Lett. **B329** (1994) 399
3. K. Abe et al., Phys. Rev. Lett. **74** (1995) 346
4. J.F. Donoghue, C.R. Nappi, Phys. Lett. **B168** (1986) 105
5. J. Gasser, H. Leutwyler, M.E. Sainio, Phys. Lett. **B253** (1991) 252
6. M. Anselmino, M.D. Scadron, Phys. Lett. **B229** (1989) 117
7. H.J. Lipkin, Phys. Lett. **B256** (1991) 284
8. J. Reifenröther et al., Phys. Lett. **B267** (1991) 299
9. C. Amsler et al., Phys. Lett. **B346** (1995) 363
10. A. Bertin et al., Phys. Lett. **B388** (1996) 450
11. Y. Lu, B.S. Zou, M.P. Locher, Z. Physik **A345** (1993) 207
12. H.J. Lipkin, B.S. Zou, Phys. Rev. **D53** (1996) 6693
13. D. Buzutu, F.M. Lev, Phys. Lett. **B329** (1994) 143
14. A.V. Anisovich, E. Klempt, Z. Physik **A354** (1996) 197
15. H.J. Besch et al., Nucl. Phys. **B70** (1974) 257
16. D.P. Barber et al., Z. Physik **C12** (1982) 1
17. H.J. Behrend et al., Nucl. Phys. **B114** (1978)
18. E. Smith et al., Measurement of the polarization of the ϕ in electroproduction, E-93-022 CEBAF proposal
19. D. Tedeschi et al., Photoproduction of ϕ mesons with linearly polarized photons, E-98-109 CEBAF proposal
20. E. Klempt, Hadron'97 Summary Talk (Expt), 7^{th} Int. Conf. Hadron Spectroscopy, S.U. Chung, H.J. Willutzki (editors), AIP 432
21. D.P. Barber et al., Z. Physik **C7** (1980) 17
22. H.Garcilazo, E.Moya de Guerra, Nucl.Phys. **A562** (1993) 521. M. Guidal, DAPNIA/SPhN-96-03T (1997)
23. M.Guidal, J.-M. Laget, M.Vanderhaeghen, Nucl.Phys. **A627** (1997) 645
24. A.I. Titov, Y. Oh, S.N. Yang, T. Morri, Phys. Rev. **C58** (1998) 2429
25. E. Klempt, Photon excitations of baryon resonances, proceedings Baryons'98, published by World Scientific
26. D. G. Cassel *et al.*, Phys. Rev. **D24**, 2787 (1981)
27. D. W. G. S. Leith, in *Electromagnetic Interactions of Hadrons*, Vol. 1, edited by A. Donnachie, G. Shaw, (Plenum Press, New York, 1978), p. 345
28. J. M. Laget, J. Korean Phys. Soc. **26**, S244 (1993)
29. P. V. Landshoff, O. Nachtmann, Z. Phys. C **35**, 405 (1987)
30. A. Donnachie, P. V. Landshoff, Nucl. Phys. **B311**, 509 (1988/1989); Phys. Lett. B **296**, 227 (1992)
31. J. R. Cudell, Nucl. Phys. **B336**, 1 (1990)
32. S. V. Goloskokov, Phys. Lett. B **315**, 459 (1993)
33. J.-M. Laget, R. Mendez-Galain, Nucl. Phys. **A581**, 397 (1995)
34. V.V.Anisovich, M.N.Kobrinsky, D.I.Melikov, A.V.Sarantsev. Nucl.Phys. **A544** (1992) 747
35. V.V.Anisovich, A.A.Anselm. Sov.Phys.Usp. **88** (1966) 117
36. A. Donnachie, P. V. Landshoff, Phys. Lett. B **185**, 403 (1987)
37. H. J. Besch, G. Hartmann, R. Kose, F. Krautschneider, W. Paul, U. Trinks, Nucl. Phys. **B70**, 257 (1974)

38. G. G. Ohlsen, Rep. Prog. Phys. **35**, 717 (1972)
39. C. Bourrely, E. Leader, J. Soffer, Phys. Rep. **59**, 95 (1980)
40. H. E. Conzett, Rep. Prog. Phys. **57**, 1 (1994)
41. F. Tabakin, Nucl. Phys. **A570**, 311c (1994); M. Pichowsky, Ç. Şavkli, F. Tabakin, Phys. Rev. C **53**, 593 (1996)
42. Ç. Şavklı, F. Tabakin, S. N. Yang, Phys. Rev. C **53**, 1132 (1996)
43. A. V. Anisovich, V. V. Anisovich, V. A. Nikonov. hep-ph/0011191